HHS Public Access

Author manuscript

Cell. Author manuscript; available in PMC 2017 February 25.

Published in final edited form as:

Cell. 2016 February 25; 164(5): 859–871. doi:10.1016/j.cell.2016.01.024.

Sialylated milk oligosaccharides promote microbiota-dependent growth in models of infant undernutrition

Mark R. Charbonneau[1,2], **David O'Donnell**[1,2], **Laura V. Blanton**[1,2], **Sarah M. Totten**[4,5], **Jasmine C. C. Davis**[4,5], **Michael J. Barratt**[1,2], **Jiye Cheng**[1,2], **Janaki Guruge**[1,2], **Michael Talcott**[6], **James R. Bain**[7,8,9], **Michael J. Muehlbauer**[7], **Olga Ilkayeva**[7], **Chao Wu**[10], **Tedd Struckmeyer**[10], **Daniela Barile**[3,5], **Charles Mangani**[11], **Josh Jorgensen**[12], **Yue-mei Fan**[13], **Kenneth Maleta**[11], **Kathryn G. Dewey**[12], **Per Ashorn**[13,14], **Christopher B. Newgard**[7,8,9], **Carlito Lebrilla**[4,5], **David A. Mills**[3,5], and **Jeffrey I. Gordon**[1,2]

[1]Center for Genome Sciences and Systems Biology, Washington University School of Medicine, St. Louis, MO 63110, USA [2]Center for Gut Microbiome and Nutrition Research, Washington University School of Medicine, St. Louis, MO 63110, USA [3]Department of Food Science and Technology, University of California at Davis, Davis, CA, 95616, USA [4]Department of Chemistry, University of California at Davis, Davis, CA, 95616, USA [5]Foods for Health Institute, University of California at Davis, Davis, CA, 95616, USA [6]Division of Comparative Medicine, Washington University School of Medicine, St. Louis, MO 63110, USA [7]Sarah W. Stedman Nutrition and Metabolism Center and Duke Molecular Physiology Institute, Duke University Medical Center, Durham, NC 27710, USA [8]Department of Medicine, Duke University Medical Center, Durham, NC 27710, USA [9]Department of Pharmacology and Cancer Biology, Duke University Medical Center, Durham, NC 27710, USA [10]Hilmar Ingredients, Hilmar Cheese Company, Hilmar, CA 95324, USA [11]College of Medicine, University of Malawi, Chichiri, Blantyre 3, Malawi [12]Department of Nutrition, University of California, Davis, CA, 95616, USA [13]Department of International Health, School of Medicine, University of Tampere, Tampere, Finland [14]Department of Paediatrics, Tampere University Hospital, Tampere, Finland

Correspondence to: jgordon@wustl.edu.

SUPPLEMENTAL INFORMATION

Supplemental information includes Extended Experimental Procedures, four figures and eight tables.

AUTHOR CONTRIBUTIONS

M.R.C., D.A.M. and J.I.G. designed the experiments; M.R.C., D.O. and M.T. generated gnotobiotic piglets; M.R.C. and J.G. produced the bacterial culture collection; L.V.B. and K.G.D. designed the M8 diet; C.W. and D.B. purified and characterized S-BMO; K.M., C.M., Y.F., J.J., K.G.D. and P.A. designed and oversaw the clinical studies; S.T. and J.C.C.D. analyzed HMO content of breast milk samples; M.R.C. and D.O. performed gnotobiotic mouse and piglet experiments; M.R.C. performed *in vitro* experiments; J.C., J.R.B., M.J.M. and O.I. performed metabolomics analyses; M.R.C. generated 16S rRNA, COPRO-Seq and microbial RNA-Seq datasets, plus draft assemblies and annotations of the genomes of cultured bacterial strains; M.R.C., M.J.B., C.B.N., C.L., D.A.M. and J.I.G. analyzed the data; M.R.C. and J.I.G wrote the paper.

ACCESSSION NUMBERS

Bacterial V4-16S rRNA, COPRO-Seq, and microbial RNA-Seq datasets plus whole genome shotgun sequencing datasets from cultured bacterial strains have been deposited in the European Nucleotide Archive (ENA) under accession PRJEB9488.

Summary

Identifying interventions that more effectively promote healthy growth of children with undernutrition is a pressing global health goal. Analysis of human milk oligosaccharides (HMOs) from 6-month postpartum mothers in two Malawian birth-cohorts revealed that sialylated HMOs are significantly less abundant in mothers with severely stunted infants. To explore this association, we colonized young germ-free mice with a consortium of bacterial strains cultured from the fecal microbiota of a 6-month old stunted Malawian infant and fed recipient animals a prototypic Malawian diet with or without purified sialylated bovine milk oligosaccharides (S-BMO). S-BMO produced a microbiota-dependent augmentation of lean body mass gain, changed bone morphology and altered liver, muscle and brain metabolism in ways indicative of a greater ability to utilize nutrients for anabolism. These effects were also documented in gnotobiotic piglets using the same consortium and Malawian diet. These preclinical models indicate a causal, microbiota-dependent relationship between S-BMO and growth promotion.

INTRODUCTION

The global burden of childhood undernutrition is great, causing 3.1 million deaths annually and accounting for 45% of all deaths under five years of age in 2011 (Black et al., 2013). Stunting, defined by a height-for-age Z-score (HAZ) below two standard deviations from the mean for a reference cohort of healthy children, is the most prevalent form of undernutrition. Stunting has lifelong consequences beyond reduced height, including impaired intellectual development (e.g., Victora et al., 2008). The causes of stunting are believed to include environmental, genetic and epigenetic factors (Martorell and Zongrone, 2012). Unfortunately, the effects of current interventions on growth, immune function and neurodevelopmental outcomes have been modest (Dewey and Adu-Afarwuah, 2008). Recent culture-independent studies of the gut microbiota from infants and children have demonstrated that the normal pattern of microbiota assembly is disrupted in children with undernutrition, leading to the proposal that disrupted microbiota development impairs healthy postnatal growth (Subramanian et al., 2014).

The World Health Organization (WHO) recommends exclusive breastfeeding for 6 months (Kramer and Kakuma, 2002). Human milk is composed of many bioactive substances, including a diverse repertoire of human milk oligosaccharides (HMOs) that may be decorated with fucose and/or sialic acid moieties (Coppa et al., 2011; Smilowitz et al., 2014). HMOs are not absorbed in the proximal gut (Engfer et al., 2000) and function as prebiotics for bacterial strains associated with numerous benefits [e.g., improved vaccine responses (Huda et al., 2014), enhanced gut barrier function (Ewaschuk et al., 2008) and protection from enteropathogen infection (Fukuda et al., 2011)].

The relationship between breast milk HMOs and the growth phenotypes of infants, particularly in populations where undernutrition is pervasive, has not been well characterized. The current study addresses this issue by first characterizing breast milk HMO content in Malawian mothers whose 6-month old infants either exhibited healthy growth or were severely stunted. Differences identified in their breast milk HMO profiles were then translated to preclinical tests of whether one difference, involving sialylated

HMOs, was causally related to growth. Germ-free mice and newborn piglets were colonized with a consortium of cultured bacterial strains isolated from the fecal microbiota of a severely stunted Malawian infant and fed a representative Malawian diet with or without the addition of sialylated bovine milk oligosaccharides (S-BMO; structurally similar to sialylated HMO). The results establish that this S-BMO preparation produces a microbiota-dependent promotion of growth and metabolic changes indicative of improved nutrient utilization in both host species. They also illustrate a generalizable preclinical pathway for characterizing the effects of diet-based interventions designed to treat and/or prevent undernutrition and its co-morbidities in infants.

RESULTS

Human milk oligosaccharide content correlates with growth in Malawian infants

Breast milk samples were collected from Malawian mothers at 6 months postpartum as part of the Lungwena Child Nutrition Intervention Study #5 (LCNI-5; Mangani et al., 2013). Samples were selected for HMO analysis from mothers whose children exhibited either healthy growth (HAZ > 0; *n*=29 mothers) or severe stunting (HAZ < −3; *n*=59). Liquid chromatography time-of-flight mass spectrometry (LC-TOF MS) detected over 50 unique oligosaccharide structures among the samples (Table S1A). HMOs containing sialic acid and/or fucose residues represented 71.8±1.5% (mean ± SEM) of total HMOs (Table S1A). Mothers of healthy infants had significantly higher concentrations of total, sialylated and fucosylated HMOs than mothers of severely stunted infants (Figure 1A). The most growth discriminatory sialylated HMO for the entire sampled LCNI-5 cohort was sialyllacto-*N*-tetraose b (LSTb), while the most discriminatory fucosylated HMOs were 2'-fucosyllactose (2'FL) and lacto-*N*-fucopentaose I (LNFP I) (Table S1A).

Mothers with a functional *FUT2* gene produce α1–2 linked fucosylated HMOs ('secretor phenotype'). As expected, the total and fucosylated HMO content of breast milk samples collected from secretor mothers in this cohort (*n*=69) was significantly higher than that of non-secretors [*n*=19; $p<0.05$, two-way ANOVA (Table S1A)]. Among non-secretor mothers, those whose children were severely stunted had HMO profiles that were significantly deficient in fucosylated and sialylated HMOs compared to milk from mothers of healthy infants (Figure 1A). The most discriminatory HMOs were sialyllacto-*N*-tetraose b, as well as the sialylated 4021b species [Neu5Ac(α2–6)Gal(β1–4)GlcNAc(β1–3)Gal(β1–4)GlcNAc(β1–3)Gal(β1–4)Glc (Table S1A)]. Among secretor mothers, no significant differences in HMO abundances were observed between those with healthy infants and those with stunted infants (Table S1A). One interpretation of these data is that some non-secretor Malawian mothers are unable to compensate for deficiencies in fucosylated HMOs through increased output of other (e.g., sialylated) HMOs, resulting in breast milk that is less supportive of healthy infant growth.

We extended our analysis of breast milk HMOs to mothers enrolled in a second birth cohort study conducted in rural Malawi (iLiNS-DYAD-M; Ashorn et al., 2015). Breast milk samples (*n*=215) were selected for HMO analysis based on infant HAZ scores at 6 months postpartum (HAZ < −2 or HAZ > 0). Similar to LCNI-5 mothers, we found that total and sialylated HMO content was significantly elevated for mothers of healthy infants (HAZ > 0;

n=70) compared to mothers of stunted infants [HAZ < −2; *n*=145 (Figure 1B, Table S1B)]. Fucosylated HMO content was not significantly enriched for mothers of healthy infants in the iLiNS-DYAD-M cohort.

For this second cohort, we also observed that breast milk from non-secretor mothers of healthy infants (*n*=20) exhibited significantly higher levels of total, fucosylated and sialylated HMOs than milk of non-secretor mothers of stunted infants (*n*=40; Figure 1B). While secretor mothers' milk displayed no significant differences in total or fucosylated HMOs between infant anthropometry bins (as observed with LCNI-5; Table S1B), sialylated HMOs were significantly elevated in milk from mothers of healthy infants (*n*=50) compared to those with stunted infants (*n*=105; $p<0.01$, Welch's t-test). These results from two independent clinical studies in Malawi raised the possibility that HMOs play an important role in infant growth.

Cultured bacterial strains from the fecal microbiota of a stunted Malawian infant

We reasoned that the hypothesis that HMOs are causally related to healthy growth could be tested preclinically in gnotobiotic animals colonized with the gut microbiota of a stunted Malawian infant and fed a Malawian diet with or without addition of bovine milk oligosaccharides (BMOs) that have structural similarities to HMOs (Aldredge et al., 2013). Colonizing germ-free animals with a genome-sequenced bacterial culture collection, generated from the fecal microbiota of an individual infant donor representing a human population of interest, is valuable for a number of reasons. Members of the collection represent the microbial exposures experienced by the host, including inheritance of microbes from the mother, and reflect selection placed on the microbiota by regional dietary practices. Importantly, the culture collection in its entirety, or subsets of the collection, can be utilized to define the contributions of bacterial strains to host biology. This is not possible when transplanting intact, uncultured communities. With these considerations in mind, we generated a collection of bacterial strains from the fecal microbiota of a severely stunted 6-month old Malawian infant (HAZ, −3.48; weight-for-height Z-score, 0.05). The collection was composed of 25 distinct strains (strains defined as isolates sharing ≥96% genome-wide nucleotide sequence similarity; Table S2A). Sequencing 16S rRNA gene amplicons from the infant's uncultured fecal microbiota revealed that 77.8% of the bacterial composition detected in the intact community (97% ID OTUs, weighted by relative abundance) was represented in the culture collection (Figure 2A).

Mapping draft genomes to the Virulence Factor Database (Chen et al., 2012) indicated that 16 strains possessed at least one known or putative virulence factor, and eight had more than three (Table S2B). The *Salmonella enterica* strain possessed homologs to 170 of the 176 virulence factors (96.6%) found in *S. enterica* subsp. *enterica* serovar Typhimurium, a pathogen in both humans and mice. The sole *E. coli* strain contained two key virulence factors associated with enteroaggregative *E. coli*: *aggR* and *aap*.

The genome content of bacterial isolates from an individual can vary substantially from laboratory strains. 22 of the 25 strains shared greater than 97% full-length 16S rRNA gene sequence identity with their closest assignable reference type strain (Figure 2B). In contrast, only six isolates shared greater than 90% overall genome nucleotide sequence similarity,

none had greater than 93% and three shared less than 40% with the reference type strain (Figure 2B).

S-BMO supplementation improves growth in young gnotobiotic mice

Since large-scale purification of HMOs from human milk is not feasible, we purified a monosaccharide- and lactose-free mixture of sialylated bovine milk oligosaccharides (S-BMO) from a commercial cheese whey stream. 3'- and 6'-sialyllactose accounted for 88% of the oligosaccharide content of S-BMO; the remaining oligosaccharides were predominantly neutral trihexoses of glucose, galactose and *N*-acetyl-glucosamine/-galactosamine (∼10.5%) and longer neutral oligosaccharides (1.5%; see Table S3A).

Dietary information for Malawian infants during the transition from exclusive breastfeeding to weaning allowed us to develop a representative Malawian diet consisting of eight principal ingredients (M8). This diet does not satisfy the recommended daily nutritional needs of humans or mice (Table S3B,C).

Groups of 5-week old male germ-free C57BL/6J mice (*n*=4–5/cage) were colonized with a single oral gavage of the defined 25-strain community. Mice were fed M8 ± S-BMO (Figure 2C). A separate group of mice received M8 supplemented with inulin [a heterogeneous mixture of fructose polymers similar to fructo-oligosaccharides commonly added to infant formulas (Bode, 2012)]. S-BMO and inulin were added separately to M8 at a level corresponding to HMO abundance in mature mother's milk (Coppa et al., 2011). The supplemented diets were isocaloric to M8 (Table S3C).

We applied shotgun sequencing of fecal DNA (COmmunity PROfiling by sequencing; COPRO-Seq), to determine colonization efficiency at strain-level resolution (McNulty et al., 2011). Colonization was defined as a strain achieving >0.1% mean relative abundance in at least one diet treatment group 44 days following initial colonization. 19 of the 25 strains (76%) colonized recipient gnotobiotic mice (Table S4A). Those that failed to colonize included both strains of *Bifidobacterium longum* subsp. *infantis*, *Klebsiella varicola*, *Peptoniphlius harei* and one strain each of *Enterococcus faecalis* and *Olsenella uli*. The strains that successfully colonized mice represent 10/11 (91%) of the bacterial genera and all four bacterial phyla that constitute the 25-member defined community. Colonization was highly reproducible among replicate animals within and across treatment groups (Figure S1A,B, Table S4A).

Body weight and composition was monitored over a 5-week period. Weight gain was significantly increased by S-BMO but not by inulin supplementation (Figure 3A). Lean body mass gain was also significantly increased by S-BMO (Figure 3B), while no significant differences in fat mass gain were observed (data not shown). These results were documented in two independent gnotobiotic mouse experiments. The observed differences in weight and lean body mass gain were not attributable to differences in food consumption, which was not significantly different between treatment groups [2.17±0.44 g/mouse/day (mean±SD) vs 2.92±0.33 g/mouse/day for control and S-BMO-treated animals, respectively; p=0.08, Students t-test]. S-BMO-associated growth promotion was also microbiota-dependent; it was not observed in germ-free animals (Figure 3C).

A previous study of germ-free and conventionally-raised mice indicated that the microbiota affects bone mass (Sjogren et al., 2012). Microcomputed tomography (μCT) of femurs revealed that, compared to controls consuming the M8 diet alone, S-BMO supplementation was associated with significant increases in cortical thickness, cortical volumetric bone mineral density (vBMD) and cortical bone volume normalized to tissue volume (BV/TV) (Figure 3D, Table S5). Histological analysis of femurs also disclosed significantly increased BV/TV in the trabecular region in mice consuming the S-BMO-supplemented diet (Figure 3D,E). No significant difference was observed in osteoclast number normalized to bone surface area (data not shown), indicating that these effects were not due to fewer osteoclasts resorbing bone. Mechanical loading is associated with a reduced medullary area in the cortical region of femur (Kodama et al., 1999). However, we observed no significant difference in cortical medullary area in the femurs of S-BMO-supplemented mice compared to controls (Table S5). This observation suggests that the increased BV/TV and vBMD associated with S-BMO treatment is not simply due to increased body weight.

Members of the distal gut microbiota respond transcriptionally to S-BMO *in vivo*

S-BMO treatment did not produce a robust change in the relative abundance of any community member over the course of the experiment other than *E. coli* (Table S4D). This strain exhibited a significantly greater relative abundance in S-BMO treated animals during the first 16 days following initial colonization (Figure 4A).

We identified bacterial strains that responded transcriptionally to S-BMO supplementation by sequencing RNA isolated from the animals' cecal contents (10.8±1.5 million reads/sample). After correction for multiple hypotheses (α=0.1), S-BMO did not produce statistically significant changes in gene expression in any of the three *Bifidobacterium* strains (*B. catenulatum*, *B. breve* and *B. bifidum*) that colonized recipient gnotobiotic mice. In addition, no genes in the *S. enterica* strain were differentially expressed with S-BMO supplementation. To rule out the possibility that the effects of S-BMO were attributable to this enteropathogen, groups of five-week old male germ-free animals were colonized with the culture collection, with or without *S. enterica*. Its removal had no significant effect on body weight or lean body mass gain (data not shown).

The two organisms that exhibited the greatest transcriptional response to S-BMO were *E. coli* and *B. fragilis* (Figure 4B). A total of 111 *E. coli* genes were differentially expressed (p<0.1, negative binomial test after Benjamini-Hochberg correction), with 110 exhibiting greater representation in the cecal meta-transcriptome of S-BMO-treated animals (Table S6). These responses represented increased gene expression, rather than increased abundance; at the time of sacrifice, there was no significant difference in this strain's relative abundance in cecal contents between groups, as determined by 16S rRNA sequencing and COPROSeq (Figure 4A, Table S4A). KEGG annotation of the set of differentially expressed *E. coli* genes revealed several pathways involved in central energy metabolism that were upregulated by S-BMO, including the TCA cycle, glycolysis/gluconeogenesis, pyruvate metabolism, galactose metabolism, purine and pyrimidine metabolism and aminoacyl-tRNA biosynthesis (Figure 4C). Although this strain contains homologs of two key virulence

factors associated with enteroaggregative *E. coli* (Table S2B), neither had detectable levels of expression in either diet context.

E. coli is not known to be a direct consumer of HMOs. We hypothesized that its response to S-BMO reflects membership in a bacterial food web, where primary consumers catabolize S-BMO and *E. coli* benefits secondarily. Members of the genus *Bacteroides* harbor arsenals of polysaccharide utilization loci (PULs), which function to import and metabolize dietary and host glycans. PULs are minimally defined by an adjacent pair of genes homologous to two *B. thetaiotaomicron* starch utilization system (Sus) genes: *susC* and *susD*. Two species of *Bacteroides*, *B. fragilis* and *B. ovatus*, were represented in the Malawian infant community that colonized recipient gnotobiotic mice. While no differences in PUL expression were documented in *B. ovatus*, several *B. fragilis* PULs exhibited differential expression with S-BMO supplementation. One upregulated PUL contains *susC* and *susD* homologs adjacent to genes encoding an *N*-acetylneuraminic acid lyase (EC4.1.3.3) and an *N*-acetylglucosamine epimerase (EC5.1.3.8; Figure 4D), consistent with this PUL being involved in S-BMO metabolism (*N*-acetylneuraminic and *N*-acetylglucosamine are major components of S-BMO; Table S3A).

Cross-feeding between *B. fragilis* and *E. coli*

These findings suggested that *B. fragilis* is a primary consumer of S-BMO, involved in a food web where *E. coli* acts as a secondary consumer. To test this notion, we incubated *B. fragilis* or *E. coli* in PBS containing S-BMO and assayed the supernatants for sialyllactose and sialic acid using ultra high performance liquid chromatography-mass spectrometry (UPLC-MS). This analysis confirmed that *B. fragilis* degraded sialyllactose, producing a concomitant increase in free sialic acid. In contrast, *E. coli* did not significantly alter the concentration of either compound under these conditions (Figure 4E).

To determine whether the products of S-BMO degradation by *B. fragilis* could support the growth of *E. coli*, S-BMO was incubated with *B. fragilis*. Subsequent growth of *E. coli* was robust in minimal medium containing the *B. fragilis*-conditioned S-BMO as the sole carbon source but minimal with unconditioned S-BMO (Figure 4F). Growth in medium containing conditioned S-BMO was also significantly increased compared to controls with sialic acid added as the sole carbon source (Figure 4F), even though *E. coli* degraded sialic acid [28.0±4.2% decrease (mean±SD) compared to uninoculated controls, $p<0.01$, Student's t-test]. These results suggest that lactose, or its constituent monomers, glucose and galactose, are the primary substrates used by *E. coli* under these conditions.

These observations raised the possibility that the microbiota-dependent growth promotion observed *in vivo* with S-BMO supplementation could be attributed either directly to primary consumers of S-BMO (e.g., *B. fragilis*) or indirectly to secondary consumers (e.g., *E. coli*). Therefore, we assessed the ability of S-BMO to promote growth of 5 week-old male gnotobiotic mice colonized with only the *B. fragilis* and *E. coli* strains. S-BMO did not produce a significant difference in growth of these mice over a 5-week period compared to M8 controls (Figure 4G). We concluded that (i) colonization of the gut *per se* is not sufficient to produce the S-BMO-enhancement of growth, and (ii) other members of the

community and/or higher-order interactions between *B. fragilis*, *E. coli* and these other members are required to mediate this growth promotion.

S-BMO supplementation modulates metabolism in host tissues

We used targeted MS/MS and GC/MS to measure the levels of a panel of 176 metabolites (Newgard et al., 2009) in liver, serum and brain obtained from S-BMO-supplemented versus M8 control mice 5 weeks after initial gavage of the 25-member bacterial culture collection. We observed significantly lower levels of medium- and long-chain acylcarnitines in the sera of non-fasted, S-BMO-treated animals compard to controls (Figure 5A); this observation was mirrored by decreases in 11 medium- and long-chain acylcarnitines and five fatty acyl CoAs in their livers (Figure S2A, Table S7A). The decreased levels of fatty acid metabolites in the liver and serum of these non-fasted mice could reflect a more normalized anabolic state. Accordingly, we documented that these animals had significantly elevated concentrations of serum triglycerides, insulin and leptin (Figure S2B–D). We also noted a trend of higher serum non-esterified fatty acids (NEFA) [0.75±0.14 mM (mean±SD) versus 0.59±0.06 mM for S-BMO-supplemented and control animals, respectively (p=0.1, Student's t-test)]. Low serum leptin levels were a major predictor of childhood mortality in a cohort of undernourished Ugandan children (Bartz et al., 2014), and leptin levels correlate with bone mineral density in women (Thomas et al., 2001).

These observations suggest that S-BMO-supplemented mice more effectively utilize dietary components for anabolism. To test the corollary that S-BMO-treated animals are better equipped to mobilize nutrients during periods of fasting, we measured metabolites in the livers and sera of mice that had been fed M8 with or without S-BMO (or inulin) and then euthanized following an 8-hour fast. The concentrations of medium- and long-chain acylcarnitines (notably C18, C18:1 and C18:2) were elevated in the sera of fasted, S-BMO-treated animals compared to M8 controls (Figure 5A, Table S7B). In addition, concentrations of 15 acylcarnitine and 29 long-chain fatty acyl CoA species were significantly higher in the livers of S-BMO-treated animals (Figure 5B, Table S7B). Similar changes were not seen in mice consuming M8 + inulin. In aggregate, our findings demonstrate a greater increment of lipid-derived metabolite concentrations in S-BMO-treated mice between the fed and fasted states than in mice fed an unsupplemented diet. This pattern is consistent with more efficient switching from anabolic storage of fat in the fed state to its oxidation in the fasted state, or increased metabolic flexibility (Muoio 2014).

No statistically significant differences were observed in cecal concentrations of organic acids or amino acids between fasted S-BMO-treated and control animals (Table S7B). We broadened our search for metabolic biomarkers associated with S-BMO-sponsored growth by performing non-targeted GC/MS analysis (Scholtens et al., 2014) of serum samples obtained at time of euthanasia from fasted mice. Orthogonal projection to latent structures discriminatory analysis (O-PLS-DA) revealed that the metabolic profile of S-BMO-treated mice clustered distinctly from that of M8 controls (Figure 5C inset); e.g., a branched-chain amino acid (BCAA) metabolite, 2-ketovaline, and a product of fatty acid oxidation, β-hydroxybutyrate, were associated with and increased by S-BMO in fasted mice (Figure 5C, Table S7D). The increase in β-hydroxybutyrate in fasted S-BMO-supplemented mice

supports our interpretation that increased fatty acid oxidation underlies the increased levels of fatty acid-derived acyl CoA and acylcarnitine species in liver and serum of these animals. The increase in a BCAA-derived metabolite also suggests that amino acids are being utilized as energy substrates in the fasted state. BCAA are also known to promote muscle protein synthesis by activating mammalian target of rapamycin (Newgard et al., 2009). This is notable given the significant augmentation in gain of lean body mass observed with S-BMO treatment (Figure 3B).

In addition to stunted growth, childhood undernutrition results in persistent deficits in cognitive development (Victora et al., 2008). Sialic acids, a group of compounds derived from neuraminic acid, including the nine-carbon monosaccharide *N*-acetylneuraminic acid (NeuAc), are integral to postnatal brain development; NeuAc is a component of gangliosides and is covalently linked to neural cell adhesion molecules (NCAMs) that mediate cell-cell interactions involved in synaptogenesis and memory (Wang and Brand-Miller, 2003). Dietary supplementation with sialylated glycoproteins has been shown to increase polysialylation of NCAM and improve memory (Wang et al., 2007a). Nontargeted UPLC/MS revealed that the metabolic profile in the brains of S-BMO-treated mice was distinct from that of control animals (Figure S3A inset, Table S7E). Interestingly, we compared the m/z feature that was most discriminatory for S-BMO-treated animals (mass 346.0546 Da; Figure S3A) to the human metabolome database (Wishart et al., 2013) and found that the compound closest in mass was an adduct of NeuAc (M+K-2H; 346.054587 Da). Applying targeted GC/MS to the same brain samples also revealed distinct metabolic profiles. Free NeuAc, inosine and adenosine were among eight metabolites identified as significantly elevated in the brains of S-BMO-treated mice (Figure S3B,C, Table S7F). Inosine treatment promotes axonal rewiring and improves behavior in animal models of traumatic brain injury (Chen et al., 2002; Dachir et al., 2014), while adenosine has both neuromodulatory and neuroprotective functions in the brain (Fredholm et al., 2005).

S-BMO supplementation promotes growth in gnotobiotic piglets

We next examined whether the observed effects of S-BMO supplementation on growth and metabolism in mice also occurred in a second mammalian species. We selected gnotobiotic piglets because the digestive physiology of swine is similar to that of humans (Miller and Ullrey, 1987). Since newborn piglets exhibit impaired gut barrier function (Wijtten et al., 2011), we excluded the eight members of the defined community with ≥3 homologs to known virulence factors in their genomes, including *E. coli* (Table S2). A group of six germ-free domestic piglets was colonized at 3 days of age with the remaining 17-strain consortium (see Table S2A) and weaned onto the M8 diet over the next seven days. At day 13 of postnatal life (day of birth defined as experimental day 1), piglets were split into control and experimental groups (n=3 piglets/group). For six days, piglets in the experimental group were fed M8 + S-BMO while control animals were fed the M8 diet alone (see Figure 6A for the experimental design; weight data were collected on days 14 through 18).

COPRO-Seq analysis of fecal samples revealed that colonization was efficient, with 14/17 (82%) of input strains detected in the piglets' fecal microbiota at >0.1% relative abundance (Table S4B). The failure of three human-derived strains (*Peptoniphilus harei* and both

strains of *Bifidobacterium longum* subsp. *infantis*) to colonize germ-free piglets in addition to germ-free mice could reflect a number of factors including their inability to thrive in the M8 diet context or restricted host specificity. As observed in mice, microbiota structure was similar between S-BMO-supplemented and control animals (Figure S1C,D, Table S4E). Piglets receiving the S-BMO-supplemented M8 diet displayed significantly greater body weight gain compared to controls (Figure 6B).

The processing of S-BMO within the gut was characterized by triple quadrupole mass spectrometry of mucosal scrapings from the proximal and distal segments of the small intestine and spiral colon (corresponds to the ascending colon in humans), plus cecal contents and feces. As expected, the concentrations of NeuAc were significantly higher in both the cecal contents and feces of S-BMO-supplemented animals (Figure 6C). Importantly, we documented a significant increase in the concentration of mucosal NeuAc in the proximal small intestine (Figure 6D), suggesting that NeuAc in S-BMO is incorporated in host glycans. This observation was site-specific; no significant differences in mucosal NeuAc concentrations were observed in the distal small intestine or spiral colon.

To investigate the effects of S-BMO on the community meta-transcriptome, we performed microbial RNA-Seq on RNA purified from cecal contents. We were unable to detect differences in gene expression for any community members using $p<0.1$ as a threshold for statistical significance (negative binomial test corrected using the Benjamini-Hochberg procedure). Relaxing this cutoff to $p<0.2$ revealed 1,482 bacterial genes that exhibited differential expression with 1,481 (99.9%) showing significantly higher expression with S-BMO treatment (Table S8). These differences are not attributable to bacterial abundance: COPRO-Seq established that S-BMO did not significantly impact the relative abundance of any colonizing strain ($p>0.05$, Student's t-test; Table S4B). Differentially expressed genes were not evenly distributed across the bacterial community; five of the community's 14 strains (*Bacteroides fragilis* MC1, *Bacteroides ovatus* MC1, *Collinsella aerofaciens* MC1, *Collinsella aerofaciens* MC2 and *Bifidobacterium catenulatum* MC1) together accounted for 1,300/1,482 (88%) of the differentially expressed genes (Table S8). Expression levels of 587 *B. fragilis* genes were significantly elevated with S-BMO-supplementation, more than any other community member. Among these 587 genes, six encode enzymes that catalyze key steps in the KEGG pathway for biosynthesis of BCAA (valine, leucine and isoleucine; Figure S4), although the concentration of BCAA in cecal contents was not significantly altered ($p>0.05$, Student's t-test; Table S7C).

Consistent with our observations in non-fasted gnotobiotic mice, the liver metabolic profiles of non-fasted, S-BMO-treated piglets exhibited significantly reduced levels of five acylcarnitine and nine fatty acyl CoA metabolites compared to controls (Figure 6E, Table S7C). In addition, we documented a striking pattern of increased amino acid concentrations, including BCAAs, in serum as well as skeletal muscle (Figure 6F,G, Table S7C). Non-fasted, S-BMO-treated piglets also displayed trends for decreased medium- and long-chain serum acylcarnitines ($p=0.12$, Student's t-test; Table S7C), increased serum triglycerides [30.33±13.05 mg/dL (mean±SD) versus 10.33±8.08 mg/dL; $p=0.08$, Student's t-test] and increased serum NEFA [0.07±0.03 mM (mean±SD) versus 0.04±0.01 mM; $p=0.2$, Student's t-test].

Finally, to determine whether the effects of S-BMO on weight gain in piglets were robust to the presence of an opportunistic enteropathogen, 3-day old animals were colonized with the 17-member bacterial community (Figure 6A; Table S2A) plus two strains of *Enterococcus faecalis* that were present in the Malawian infant's 25-member culture collection. The genomes of these two strains, *E. faecalis* MC1 and MC2, contain homologs to 20 and 22 genes, respectively, present in the Virulence Factor Database for the pathogenic *E. faecalis* strain V583 (Table S2B). Gnotobiotic piglets were weaned onto the M8 diet by experimental day 12. On day 15, animals were split into experimental and control groups (n=3 and 4, respectively), and for a period of five days, piglets in the experimental group were fed the M8 diet supplemented with S-BMO. Control animals were fed unsupplemented M8. COPRO-Seq of fecal samples, collected on day 18 disclosed that 14/19 (74%) of the input strains, including both strains of *E. faecalis*, colonized the recipient piglets (Table S4C). S-BMO supplemented piglets gained significantly more weight over the treatment period than unsupplemented controls despite the presence of these two *E. faecalis* strains ($p<0.01$, repeated measures, two-way ANOVA; Figure 6H).

Together, these results led us to conclude that the effects of S-BMO supplementation on weight gain and metabolic phenotypes are a shared feature of gnotobiotic piglets and mice and that these changes reflect, at least in part, improved utilization of dietary components. Furthermore, the fact that S-BMO promoted growth in the absence of *E. coli* provided additional evidence that other members of the microbiota and/or their higher order interactions are necessary to mediate these effects.

DISCUSSION

The data presented here from two separate studies of undernutrition in Malawi indicate that the breast milk of mothers whose children exhibit growth faltering contains lower levels of HMOs, including sialylated glycans, compared to milk from mothers of healthy infants. Sialic acid-containing oligosaccharides are present at up to 20-fold higher levels in mature human milk compared to mature bovine milk (Tao et al, 2009; Wang et al, 2001). As a result, existing bovine milk-based infant formulas and complementary/therapeutic foods used to treat undernutrition are deficient in these important human milk components. We have used two gnotobiotic animal models, each colonized with a collection of bacterial strains cultured from a single stunted Malawian infant and fed a prototypic Malawian diet, to show that a purified preparation of sialylated bovine milk oligosaccharides resembling the sialylated HMOs which are depleted in the breast milk of mothers with stunted infants produces beneficial, microbiota-dependent effects on growth and metabolism.

The brains of breastfed infants possess higher levels of ganglioside- and glycoprotein-bound sialic acid than the brains of formula-fed infants (Wang and Brand-Miller, 2003), consistent with the higher sialic acid content of breast milk compared to bovine milk-based infant formulas (Wang et al., 2001). Although the liver can synthesize sialic acid *de novo* from glucose, the activity of the limiting enzyme, UDP-*N*-acetylglucosamine-2-epimerase, is low during the neonatal period (Gal et al., 1997), suggesting that in the absence of human milk, sialic acid may be a limiting resource at the time of rapid postnatal brain development. Our finding that dietary S-BMO supplementation of gnotobiotic mice, harboring gut microbial

community members from an undernourished Malawian infant, leads to elevated levels of NeuAc in the brain indicates that S-BMO can function as a supplementary source of bioavailable sialic acid.

In addition to neural development, sialic acid may play a role in healthy growth of the musculoskeletal system. S-BMO increased bone cortical thickness and trabecular bone volume in young gnotobiotic mice. The underlying mechanisms need to be investigated, but this observation has a clinical correlate; studies in Uganda reported reductions in fibular bone width in 3.5- to 7.5-year old children who exhibited low body weight during their first 2 years of postnatal life (McFie and Welbourn, 1962). Moreover, studies of a mouse model of myopathy in which a bifunctional rate-limiting enzyme in sialic acid biosynthesis (*Gne*) is mutated, showed that addition of 6'-sialyllactose to the animals' drinking water led to increased muscle mass and improved contractility (Yonekawa et al., 2014).

Our results indicate that orally administered S-BMO restores normal substrate utilization patterns, most notably (i) a strong activation of fatty acid oxidation in fasting, as reflected by increased levels of acylcarnitines, acyl CoAs and the fatty acid oxidation end product β-hydroxybutyrate, and (ii) a pattern consistent with enhanced anabolic metabolism of lipids in the fed state, including increases in triglycerides and insulin, and decreased levels of fatty acid oxidation intermediates. Additional studies are needed to define how products of microbial biotransformation of S-BMO impact energy balance and host metabolism in ways that promote total body weight and lean body mass gain.

Our findings demonstrate that specific bacterial members of the gut microbiota obtained from an undernourished Malawian infant are able to metabolize S-BMO-derived sialyllactose to its constituent monosaccharides. These monosaccharides are available for utilization by the host as well as members of the microbiota, both mutualistic and pathogenic. The latter includes pathogenic *E. coli* that are unable to harvest sialic acids themselves from host glycans or dietary sources (Almagro-Moreno and Boyd, 2009). Therefore, it is important to consider that the presence of primary consumers of sialylated oligosaccharides may create opportunities for enteropathogens to achieve a fitness benefit that could have deleterious effects on the host (Ng et al., 2013). These findings encourage mindfulness with respect to balancing potential benefits and risks when designing gut microbiota-directed clinical trials involving milk oligosaccharides.

While our analysis of breast milk specimens from Malawian mothers disclosed an association between HMO abundance and composition and infant growth, additional time-series studies of maternal-infant dyads from Malawi and other countries are needed to determine the extent to which differences in maternal HMO composition and variations in infant microbiota structure and function (e.g., the capacity to metabolize HMOs), correlate with infant growth outcomes. Nonetheless, gnotobiotic models of the type we describe can play important roles in characterizing oligosaccharides that are structurally similar to HMOs. They provide a means to (i) elucidate their mechanisms of action, including those that underlie effects on host metabolism that would otherwise be difficult or impossible to glean from non-invasive human studies, especially those involving infants, (ii) define the generalizability of their effects in the context of gut microbiota from different human donors

representing different geographic locations and dietary practices, and (iii) identify clinically translatable microbial and host biomarkers related to mechanism and safety. If additional human studies provide evidence for a significant association between breast milk HMO composition, infant gut microbiota configurations and growth outcomes, then results of the type described by (i)-(iii) should help inform the design of proof of concept clinical studies that test the efficacy and safety of approaches such as S-BMO supplementation for improving growth outcomes in undernourished infants and children.

EXPERIMENTAL PROCEDURES

Human studies

Human studies were conducted with the approval of institutional review boards from the University of Malawi, Pirkanmaa Hospital (Finland) and Washington University School of Medicine in St. Louis. The mothers and infants included in this study were enrolled in two randomized, controlled, single-blind, parallel group clinical trials, LCNI-5 and iLiNS-DYAD-M (ClinicalTrials.gov identifiers: NCT00524446 and NCT01239693). See Extended Experimental Procedures for additional information.

Clonally arrayed culture collection

The 25-member clonally arrayed culture collection was produced from a frozen fecal sample collected from a severely stunted 6-month old Malawian infant [patient ID h264A in Yatsunenko et al. (2012)]. For detailed information relating to bacterial isolation, plus genome sequencing, assembly and annotation see Extended Experimental Procedures.

Purification and compositional analysis of S-BMO

S-BMO was purified from commercially available whey permeate using a series of ultrafiltration and chromatographic steps described in Extended Experimental Procedures.

Design and preparation of the Malawi 8 (M8) diet

This diet was formulated based on a dietary survey of the complementary feeding practices of 43 nine-month old Malawian infants and children enrolled in the iLiNS-DOSE clinical study (#NCT00945698) that took place in the Mangochi district of Malawi. See Extended Experimental Procedures for details.

Studies involving gnotobiotic mice

All gnotobiotic mouse experiments were performed using protocols approved by the Washington University Animal Studies Committee. Male germ-free C57Bl/6J mice were maintained in sterile, flexible plastic gnotobiotic isolators. Mice received a single oral gavage of the complete 25-member culture collection or subsets of the collection 3 days after initiation of one of the M8-based diets. For additional information, see Extended Experimental Procedures.

16S rRNA gene sequencing of fecal microbiota

Multiplex sequencing of barcoded bacterial 16S rRNA amplicons generated from fecal microbiota samples was performed using an Illumina MiSeq instrument. Taxonomic assignments were made with the Ribosomal Database Project (RDP) version 2.4 classifier (Wang et al., 2007b). See Extended Experimental Procedures for detailed information about sample preparation, PCR conditions, multiplex sequencing and analysis of the resulting datasets.

Microbial RNA-Seq

Multiplex microbial cDNA sequencing was performed using Illumina Hi-Seq2000, MiSeq and NextSeq instruments. Reads were mapped to genes in a custom database of 25 draft genomes of the strains included in the defined Malawian infant bacterial community. Read counts were normalized and analyzed with DESeq (Anders and Huber, 2010). See Extended Experimental Procedures for additional information.

Mass spectroscopy

Tissue samples were collected from gnotobiotic animals at time of euthanasia, frozen immediately in liquid nitrogen and stored at −80°C. In preparation for GC/MS, UPLC/MS, and MS/MS analyses, samples were homogenized in 50% aqueous acetonitrile containing 0.3% formic acid (50 mg wet weight tissue/mL solution). See Extended Experimental Procedures for details about analytic methods.

Gnotobiotic piglets

All experiments were performed under the close supervision of a veterinarian using protocols approved by the Washington University Animal Studies Committee. For detailed procedures relating to the derivation of germ-free piglets and experimental design, see Extended Experimental Procedures.

Supplementary Material

Refer to Web version on PubMed Central for supplementary material.

Acknowledgments

We are grateful to Sabrina Wagoner, Maria Karlsson, Justin Serugo, Siddarth Venkatesh, Jeanette Gehrig and Josh Sommovilla for assistance with gnotobiotic mouse and piglet husbandry, Jeremiah Faith for assistance generating the culture collection, plus Marty Meier, Su Deng, Jessica Hoisington-Lopez, Paras Vora and Daniel Leib for superb technical assistance. J.I.G. is a co-founder of Matatu, Inc., a company characterizing the role of diet-by-microbiota interactions in animal health. D.A.M., D.B. and C.B. are co-founders of Evolve Biosystems, Inc., a company focused on diet-based manipulation of the gut microbiota.

This work was supported in part by grants from the Bill & Melinda Gates Foundation and the NIH (DK30292, DK70977, P30 AR057235), with additional funding from USAID (AID-OAA-A-12-00005). Data management and statistical analysis for the iILNS-DYAD-M clinical study were supported by grants from the Academy of Finland (252075) and the Medical Research Fund of Tampere University Hospital (9M004).

REFERENCES

Aldredge DL, Geronimo MR, Hua SS, Nwosu CC, Lebrilla CB, Barile D. Annotation and structural elucidation of bovine milk oligosaccharides and determination of novel fucosylated structures. Glycobiology. 2013; 23:664–676. [PubMed: 23436288]

Almagro-Moreno S, Boyd EF. Sialic acid catabolism confers a competitive advantage to pathogenic vibrio cholerae in the mouse intestine. Infect Immun. 2009; 77:3807–3816. [PubMed: 19564383]

Anders S, Huber W. Differential expression analysis for sequence count data. Genome Biol. 2010; 11:R106. [PubMed: 20979621]

Ashorn P, Alho L, Ashorn U, Cheung YB, Dewey KG, Harjunmaa U, Lartey A, Nkhoma M, Phiri N, Phuka J, et al. The impact of lipid-based nutrient supplement provision to pregnant women on newborn size in rural Malawi: A randomised controlled trial. Am J Clin Nutr. 2015; 101:387–397. [PubMed: 25646337]

Bartz S, Mody A, Hornik C, Bain J, Muehlbauer M, Kiyimba T, Kiboneka E, Stevens R, Bartlett J, St Peter JV, et al. Severe acute malnutrition in childhood: hormonal and metabolic status at presentation, response to treatment, and predictors of mortality. J Clin Endocr Metab. 2014; 99:2128–2137. [PubMed: 24606092]

Black RE, Victora CG, Walker SP, Bhutta ZA, Christian P, de Onis M, Ezzati M, Grantham-McGregor S, Katz J, Martorell R, et al. Maternal and child undernutrition and overweight in low-income and middle-income countries. Lancet. 2013; 382:427–451. [PubMed: 23746772]

Bode L. Human milk oligosaccharides: every baby needs a sugar mama. Glycobiology. 2012; 22:1147–1162. [PubMed: 22513036]

Chen L, Xiong Z, Sun L, Yang J, Jin Q. VFDB 2012 update: toward the genetic diversity and molecular evolution of bacterial virulence factors. Nucleic Acids Res. 2012; 40:D641–D645. [PubMed: 22067448]

Chen P, Goldberg DE, Kolb B, Lanser M, Benowitz LI. Inosine induces axonal rewiring and improves behavioral outcome after stroke. Proc Natl Acad Sci USA. 2002; 99:9031–9036. [PubMed: 12084941]

Coppa GV, Gabrielli O, Zampini L, Galeazzi T, Ficcadenti A, Padella L, Santoro L, Soldi S, Carlucci A, Bertino E, et al. Oligosaccharides in 4 different milk groups, Bifidobacteria, and Ruminococcus obeum. J Pediatr Gastr Nutr. 2011; 53:80–87.

Dachir S, Shabashov D, Trembovler V, Alexandrovich AG, Benowitz LI, Shohami E. Inosine improves functional recovery after experimental traumatic brain injury. Brain Res. 2014; 1555:78–88. [PubMed: 24502983]

Dewey KG, Adu-Afarwuah S. Systematic review of the efficacy and effectiveness of complentary feeding interventions in developing countries. Matern Child Nutr. 2008; 4:24–85. [PubMed: 18289157]

Engfer MB, Stahl B, Finke B, Sawatzki G, Danial H. Human milk oligosaccharides are resistant to enzymatic hydrolysis in the upper gastrointestinal tract. Am J Clin Nutr. 2000; 71:1589–1596. [PubMed: 10837303]

Ewaschuk JB, Diaz H, Meddings L, Diederichs B, Dmytrash A, Backer J, Looijer-van Langen M, Madsen KL. Secreted bioactive factors from Bifidobacterium infantis enhance epithelial cell barrier function. Am J Physiol Gastroenterol Liver. 2008; 295:G1025–G1034.

Fredholm BB, Chen JF, Masino SA, Vaugeois JM. Actions of adenosine at its receptors in the CNS: insights from knockouts and drugs. Annu Rev Pharmacol. 2005; 45:385–412.

Fukuda S, Toh H, Hase K, Oshima K, Nakanishi Y, Yoshimura K, Tobe T, Clarke JM, Topping DL, Suzuki T, et al. Bifidobacteria can protect from enteropathogenic infection through production of acetate. Nature. 2011; 469:543–547. [PubMed: 21270894]

Gal B, Ruano MJ, Puente R, Garcia-Pardo LA, Rueda R, Gil A, Hueso P. Delevopment changes in UDP-N-acetylglucosamine 2-epimerase activity of rat and guinea-pig liver. Comp Biochem Physiol B. 1997; 118:13–15. [PubMed: 9417989]

Huda MS, Lewis Z, Kalanetra KM, Rashid M, Ahmad SM, Raqib R, Qadra F, Underwood MA, Mills DA, Stephensen CB. Stool microbiota and vaccine responses of infants. Pediatrics. 2014; 134:362–372.

Kodama Y, Dimai H, Wergedal J, Sheng M, Malpe R, Kutilek S, Beamer W, Donahue L, Rosen C, Baylink D, et al. Cortical tibial bone volume in two strains of mice: effects of sciatic neurectomy and genetic regulation of bone response to mechanical loading. Bone. 1999; 25:183–190. [PubMed: 10456383]

Kramer MS, Kakuma R. Optimal duration of exclusive breastfeeding. Cochrane Db Syst Rev. 2002; 8

Mangani C, Maleta K, Phuka J, Cheung YB, Thakwalakwa C, Dewey K, Manary M, Puumalainen T, Ashorn P. Effect of complementary feeding with lipid-based nutrient supplements and corn-soy blend on the incidence of stunting and linear growth among 6- to 18-month-old infants and children in rural Malawi. Matern Child Nutr. 2013 Jun 25.

Martorell R, Zongrone A. Intergenerational influences on child growth and undernutrition. Paediatr Perinat Ep. 2012; 26(Suppl 1):302–314.

McFie J, Welbourn HF. Effect of malnutrition in infancy on the development of bone, muscle and fat. J. Nutr. 1962; 76:97–105.

McNulty N, Yatsunenko T, Hsiao A, Faith J, Muegge B, Goodman A, Henrissat B, Oozeer R, Cools-Portier S, Gobert G, et al. The impact of a consortium of fermented milk strains on the gut microbiome of gnotobiotic mice and monozygotic twins. Sci Transl Med. 2011; 3:106ra106.

Miller E, Ullrey D. The pig as a model for human nutrition. Ann Rev Nutr. 1987; 7:361–382. [PubMed: 3300739]

Muoio DM. Metabolic inflexibility: when mitochondrial indecision leads to metabolic gridlock. Cell. 2014; 159:1253–1262. [PubMed: 25480291]

Newgard CB, An J, Bain JR, Muehlbauer MJ, Stevens RD, Lien LF, Haqq AM, Shah SH, Arolotto M, Slentz CA, et al. A branched-chain amino acid-related metabolic signature that differentiates obese and lean humans and contributes to insulin resistance. Cell Metab. 2009; 9:311–326. [PubMed: 19356713]

Ng KM, Ferreyra JA, Higginbottom SK, Lynch JB, Kashyap PC, Gopinath S, Naidu N, Choudhury B, Weimer BC, Monack DM, et al. Microbiota-liberated host sugars facilitate post-antibiotic expansion of enteric pathogens. Nature. 2013; 502:96–99. [PubMed: 23995682]

Scholtens DM, Muehlbauer MJ, Daya NR, Stevens RD, Dyer AR, Lower LP, Metzger BE, Newgard CB, Bain JR, Lowe WL. Metabolomics reveals broad-scale metabolic perturbations in hyperglycemic mothers during pregnancy. Diabetes Care. 2014; 37:158–166. [PubMed: 23990511]

Sjogren K, Engdahl C, Henning P, Lerner UH, Tremaroli V, Lagerquist MK, Backhed F, Ohlsson C. The gut microbiota regulates bone mass in mice. J Bone Miner Res. 2012; 27:1357–1367. [PubMed: 22407806]

Smilowitz JT, Lebrilla CB, Mills DA, German JB, Freeman SL. Breast milk oligosaccharides: structure function relationships in the neonate. Ann Rev Nutr. 2014; 34:143–169. [PubMed: 24850388]

Subramanian S, Huq S, Yatsunenko T, Haque R, Mahfuz M, Alam MA, Benezra A, DeStefano J, Meier MF, Muegge BD, et al. Persistent gut microbiota immaturity in malnourished Bangladeshi children. Nature. 2014; 510:417–421. [PubMed: 24896187]

Tao N, DePeters EJ, German JB, Grimm R, Lebrilla CB. Variations in bovine milk oligosaccharides during early and middle lactation stages analyzed by high-performance liquid chromatography-chip/mass spectrometry. J Dairy Sci. 2009; 92:2991–3001. [PubMed: 19528576]

Thomas T, Burguera B, Melton LJ, Atkinson EJ, O'fallon WM, Riggs BL, Khosla S. Role of serum leptin, insulin, and estrogen levels as potential mediators of the relationship between fat mass and bone mineral density in men versus women. Bone. 2001; 29:114–120. [PubMed: 11502471]

Victora CG, Adair L, Fall C, Hallal PC, Martorell R, Richter L, Sachdev HS. Maternal and child undernutrition: consequences for adult health and human capital. Lancet. 2008; 371:340–357. [PubMed: 18206223]

Wang B, Brand-Miller J. The role and potential of sialic acid in human nutrition. Eur J Clin Nutr. 2003; 57:1351–1369. [PubMed: 14576748]

Wang B, Brand-Miller J, McVeagh P, Petocz P. Concentration and distribution of sialic acid in human milk and infant formulas. Am J Clin Nutr. 2001; 74:510–515. [PubMed: 11566650]

Wang B, Yu B, Karim M, Hu H, Sun Y, McGreevy P, Petocz P, Held S, Brand-Miller J. Dietary sialic acid supplementation improves learning and memory in piglets. Am J Clin Nutr. 2007a; 85:561–569. [PubMed: 17284758]

Wang Q, Garrity GM, Tiedje JM, Cole JR. Naive Bayesian classifier for rapid assignment of rRNA sequences into the new bacterial taxonomy. Appl Environ Microb. 2007b; 73:5261–5267.

Wijtten PJ, van der Meulen J, Verstegen MW. Intestinal barrier function and absorption in pigs after weaning: a review. Brit J Nutr. 2011; 105:967–981. [PubMed: 21303573]

Wishart DS, Jewison T, Guo AC, Wilson M, Knox C, Liu Y, Djoumbou Y, Mandal R, Aziat F, Dong E, et al. HMDB 3.0--The Human Metabolome Database in 2013. Nucleic Acids Res. 2013; 41:D801–D807. [PubMed: 23161693]

Yatsunenko T, Rey FE, Manary MJ, Trehan I, Dominguez-Bello MG, Contreras M, Magris M, Hidalgo G, Baldassano RN, Anokhin AP, et al. Human gut microbiome viewed across age and geography. Nature. 2012; 486:222–227. [PubMed: 22699611]

Yonekawa T, Malicdan MC, Cho A, Hayashi YK, Nonaka I, Mine T, Yamamoto T, Nishino I, Noguchi S. Sialyllactose ameliorates myopathic phenotypes in symptomatic GNE myopathy model mice. Brain. 2014; 137:2670–2679. [PubMed: 25062695]

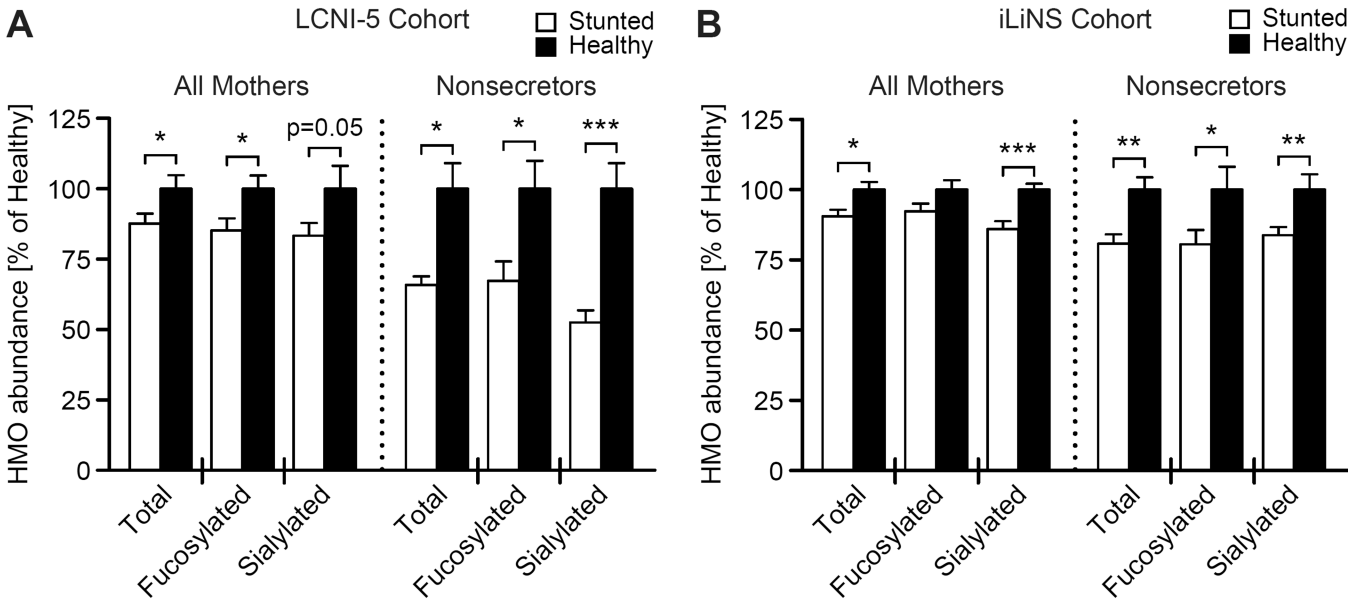

Figure 1. HMOs are more abundant in breast milk of Malawian mothers with healthy infants

(**A,B**) Abundance of total, fucosylated and sialylated HMOs present in breast milk of Malawian mothers collected from the LCNI-5 cohort (*n*=88 mothers, panel **A**) and iLiNS-DYAD-M cohort (*n*=215 mothers, panel **B**) 6 months postpartum, binned by anthropometry of their infants (LCNI-5 healthy, HAZ>0; stunted, HAZ<- 3; iLiNS-DYAD-M healthy, HAZ>0; stunted, HAZ< −2). HMO abundance values correspond to LC-TOF MS spectral abundance (mean±SEM), normalized to the mean abundance of samples assigned to the healthy bin for each respective comparison. **p*<0.05, ***p*<0.01, ****p*<0.001 (two-tailed, Welch's t-test). See also Table S1.

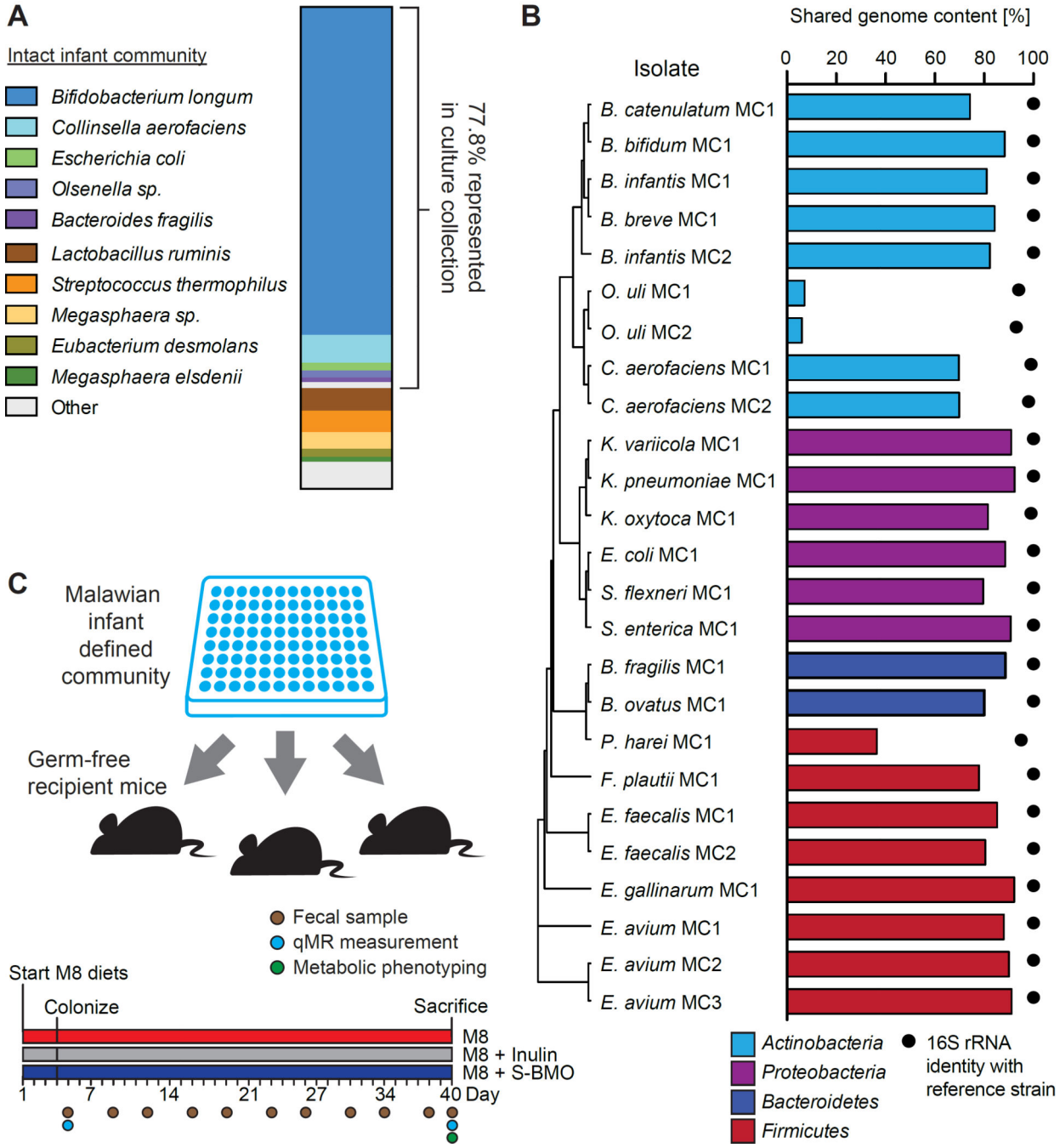

Figure 2. Cultured bacterial strain collection generated from the fecal microbiota of a 6-month old stunted Malawian infant

(**A**) Taxonomic representation of 97% ID OTUs in the intact, uncultured infant fecal sample from which the culture collection was generated. (**B**) Comparison of culture collection strains and representative type strains. Black dots indicate percent identity between full-length 16S rRNA gene sequences from each strain and its most similar reference type strain's 16S rRNA sequence. Bars indicate percent nucleotide sequence similarity between the strain's *de novo* assembled genome and its most similar type strain's genome. Strains are

clustered by Euclidean distance between full-length 16S rRNA gene sequences. (**C**) Design of gnotobiotic mouse experiments. See also Table S2.

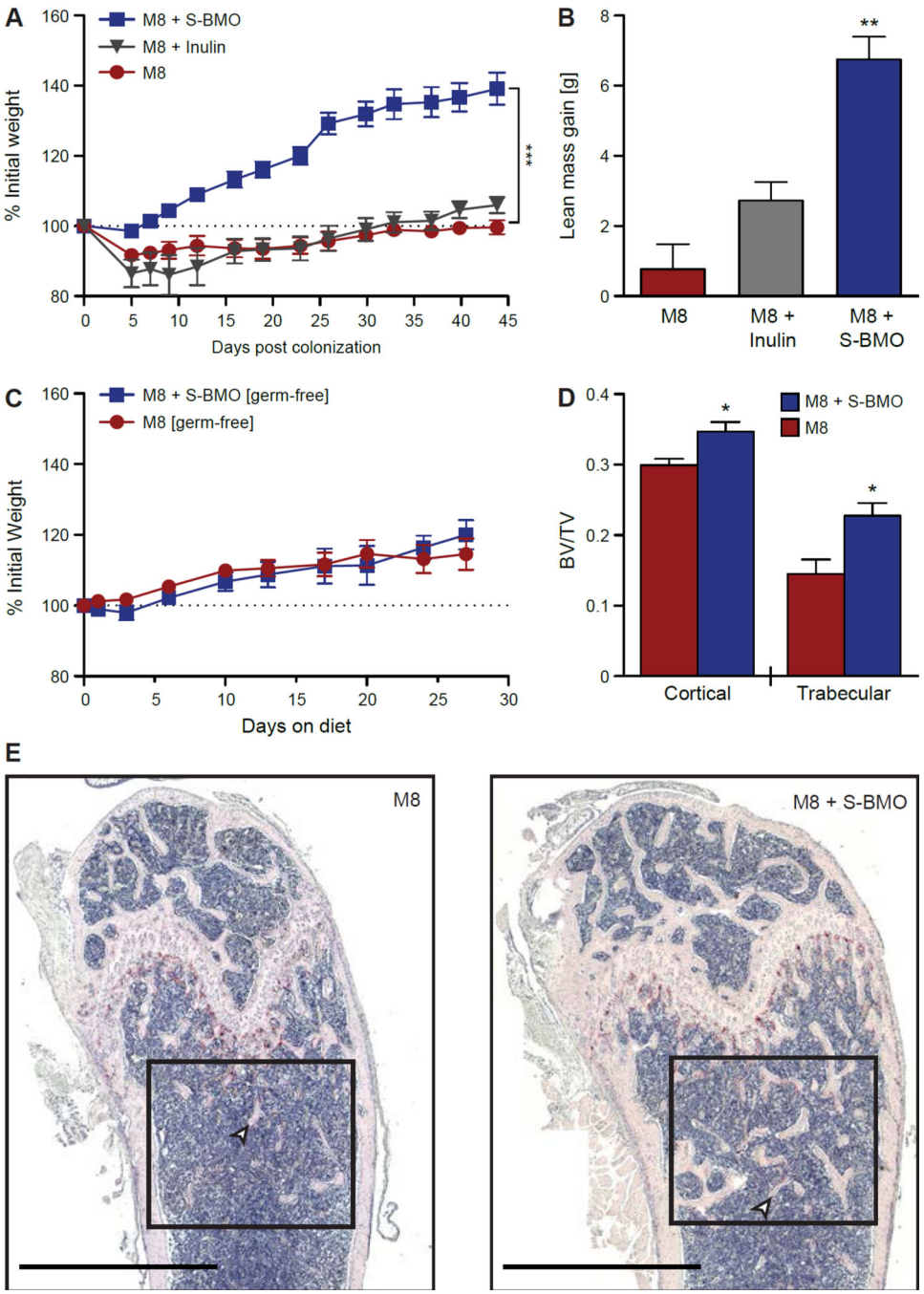

Figure 3. S-BMO promotes growth in gnotobiotic mice harboring the Malawian infant culture collection and fed a prototypic Malawian diet

(**A**) Weight gain of mice over time normalized to body weight at the time of colonization. (**B**) Lean body mass gain 44 days after colonization of mice fed M8 ± inulin or S-BMO. (**C**) Weight gain over time of germ-free mice fed M8±S-BMO for 4 weeks (normalized to weight at 5 weeks of age). (**D**) Cortical and trabecular bone volume/tissue volume (BV/TV; TV = cortical area + medullary area). (**E**) Representative histomorphometry images of femurs from mice colonized with the culture collection and fed M8 ± S-BMO. Black boxes

highlight the trabecular region of interest, and arrowheads point to examples of trabeculae. Scale bars, 1 mm. For (**A**), ***p<0.001, two-way, repeated measures ANOVA. For (**B**) and (**D**), *p<0.05, **p<0.01 two-tailed, unpaired Student's t-test. All values are represented as mean±SEM, and all comparisons are made to M8 controls. See also Figure S1 and Table S5.

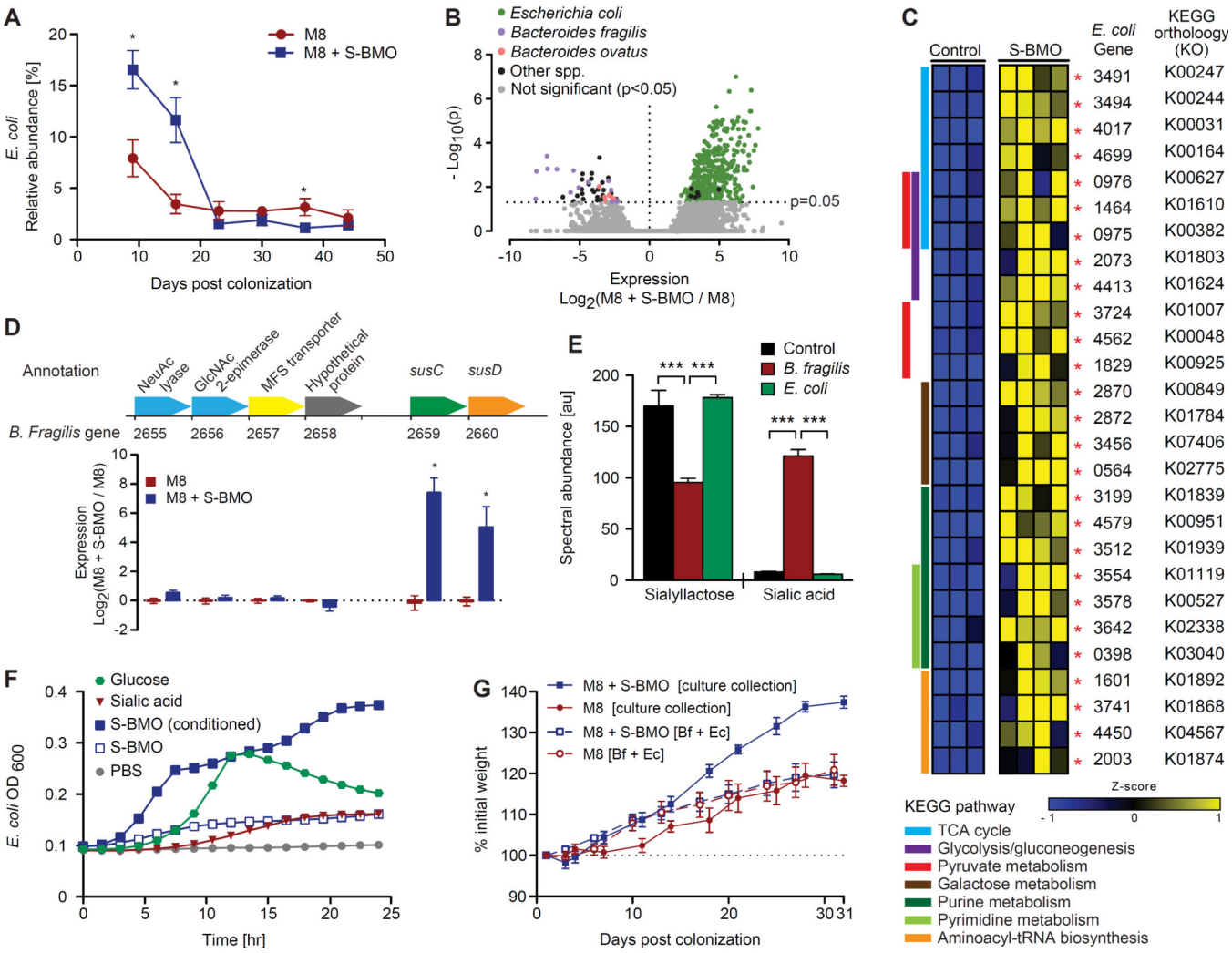

Figure 4. Members of the gut microbiota respond transcriptionally to S-BMO *in vivo* and degrade S-BMO *in vitro*

(**A**) Relative abundance of *E. coli* (mean±SEM) over time in the fecal microbiota of gnotobiotic mice colonized with the stunted Malawian infant's culture collection and fed M8 ± S-BMO. **p*<0.05 two-tailed, unpaired Student's t-test. (**B**) Volcano plot of bacterial gene expression in the cecal microbiota of gnotobiotic mice. Expression is plotted on the x-axis as the $\log_2$ fold difference between S-BMO-supplemented mice and unsupplemented mice. Significantly up- or downregulated genes are labeled in black or by bacterial species of origin. $-\text{Log}_{10}$(*p*-values) are plotted on the y-axis (Benjamini-Hochberg corrected negative binomial test). (**C**) Heatmap of select differentially expressed *E. coli* genes, grouped by KEGG functional pathway (see Table S6 for a full list). Red asterisks denote that differences in expression are statistically significant after Benjamini-Hochberg correction for multiple hypotheses (α=0.1). (**D**) Effects of S-BMO on expression of genes in a *B. fragilis* PUL. Expression is plotted on the y-axis as the $\log_2$ fold difference (mean±SEM) between S-BMO-supplemented and control mice. **p*<0.05, ***p*<0.01 (two-tailed, unpaired Student's t-test). (**E**) Abundance (mean±SEM) of siallyllactose and sialic acid in *E. coli* or *B. fragilis* monoculture supernatants after a 24-hour incubation with 5% S-BMO. Control incubations

contained uninoculated PBS buffer. ***p<0.001 two-tailed, unpaired Student's t-test. (**F**) OD_{600} (mean±SEM) of *E. coli* grown in minimal medium containing various single carbon sources. 'Conditioned S-BMO' refers to filter-sterilized supernatant from a 24-hour monoculture of *B. fragilis* with S-BMO. (**G**) Mouse weights (mean±SEM), normalized to values at time of colonization with the entire Malawian infant culture collection or with only *B. fragilis* and *E. coli* (Bf + Ec). Mice were fed M8 ± S-BMO (n=5 mice/group).

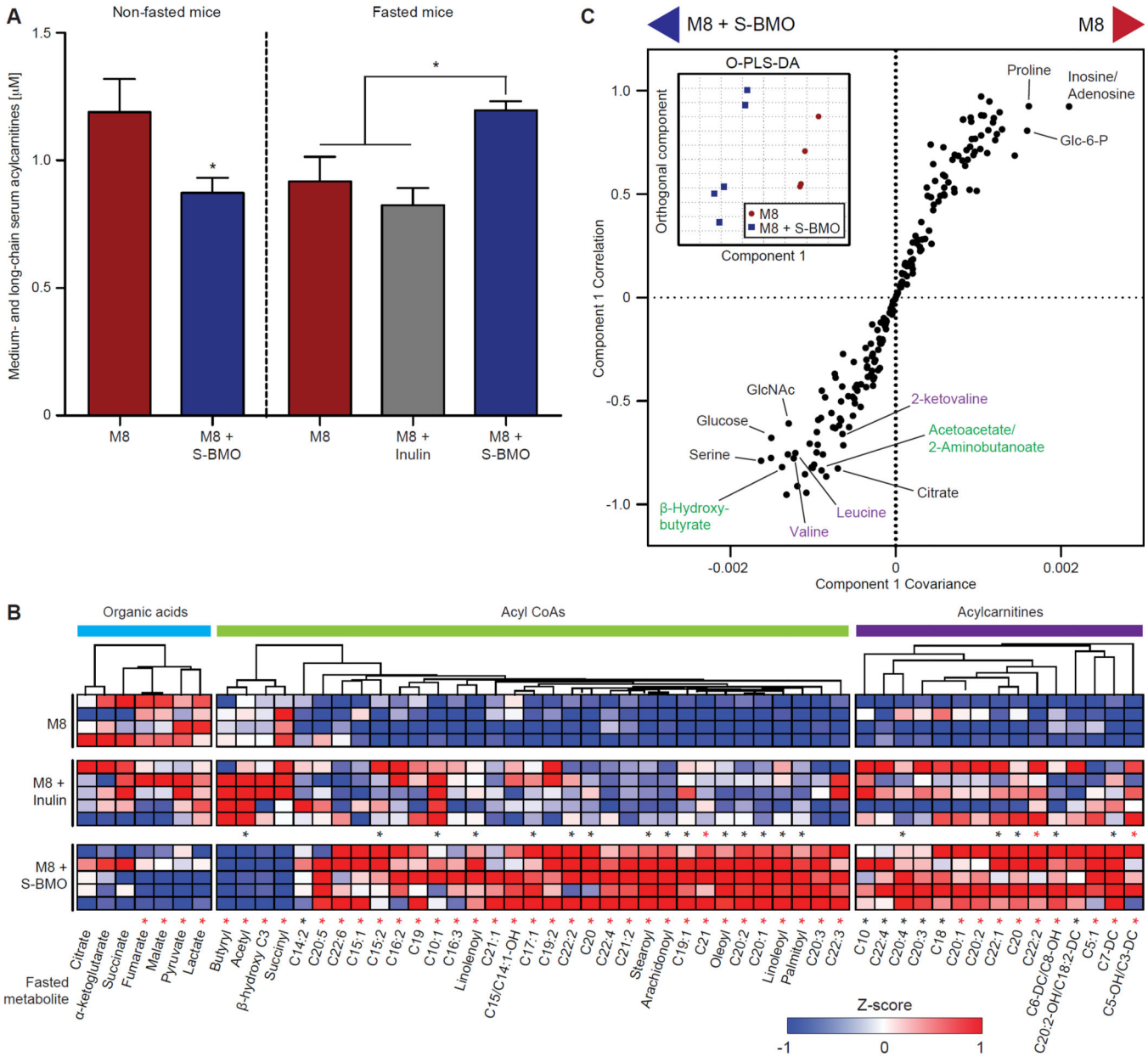

Figure 5. S-BMO supplementation alters levels of serum and liver metabolites in gnotobiotic mice

(**A**) Total concentrations of medium- and long-chain serum acylcarnitines (chain length ≥10) in fasted or non-fasted gnotobiotic mice fed M8 ± S-BMO or inulin (mean±SEM values shown). *p<0.05, Student's t-test. (**B**) Liver metabolites whose concentrations are impacted by S-BMO-treatment in fasted mice. Rows represent replicate mice, grouped by dietary treatment. Columns represent individual metabolites whose concentrations are represented as Z-scores. *p<0.05 (two-tailed, unpaired Student's t-test). All comparisons are made to controls. Red asterisks represent significant differences between groups after Benjamini-Hochberg correction for multiple hypotheses (α=0.1). See Table S7A,B for concentrations of all measured metabolites. (**C**) O-PLS-DA score plot (inset) and O-PLS-DA S-plot of

fasted serum metabolites in gnotobiotic mice fed M8 ± S-BMO. Metabolites highlighted in purple are branched-chain amino acid metabolites while those in green are ketone body metabolites. See also Figure S2 and Figure S3.

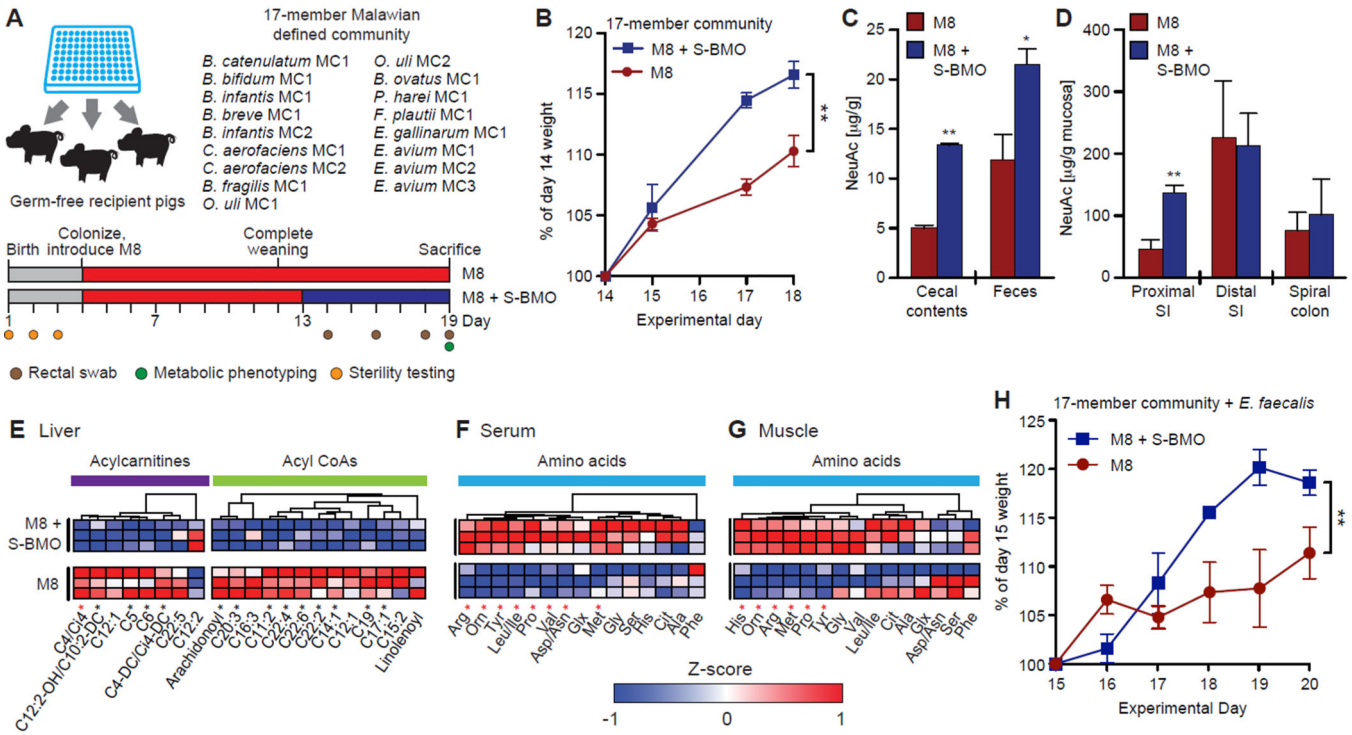

Figure 6. S-BMO modulates growth and metabolism in gnotobiotic piglets

(**A**) Experimental design. The treatment group was fed M8+S-BMO (blue bars) while controls were fed the M8 diet alone (red bars). (**B**) Weight gain normalized to body weight at postnatal day 14 (mean±SEM). ***p*<0.01, two-way, repeated measures ANOVA. (**C,D**) *N*-acetylneuraminic acid (NeuAc) concentrations in cecal contents and feces (panel **C**), as well as in proximal and distal small intestine (SI) and spiral colon mucosa (panel **D**), harvested from gnotobiotic piglets fed M8±S-BMO. **p*<0.05, ***p*<0.01 two-tailed, unpaired Student's t-test. (**E**) Heatmap displaying acylcarnitine and fatty acyl CoA concentrations in the livers of non-fasted gnotobiotic piglets. (**F,G**) Amino acid concentrations in (**F**) serum and (**G**) skeletal muscle obtained from non-fasted gnotobiotic piglets. In panels **E,F**, columns represent individual metabolites, and rows represent replicate gnotobiotic piglets, grouped by treatment. **p*<0.05 (two-tailed, unpaired Student's t-test). Metabolite concentrations are displayed as Z-scores (normalized by column). Red asterisks denote statistical significance after Benjamini-Hochberg correction (α=0.1; all comparisons are made to M8 controls). (**H**) Weight gain normalized to body weight at postnatal day 15 (mean±SEM) in gnotobiotic piglets colonized with the 17-member consortium used in panel **B** but with the addition of two strains of *Enterococcus faecalis* (*E. faecalis* MC1 and *E. faecalis* MC2), ***p*<0.01, two-way, repeated measures ANOVA. See also Figure S1, Figure S6, Table S7C and Table S8